A Printable Optical Time-Temperature Integrator Based on Shape Memory in a Chiral Nematic Polymer Network

Dylan J. D. Davies, Antonio R. Vaccaro, Stephen M. Morris, Nicole Herzer, Albertus P. H. J. Schenning, and Cees W. M. Bastiaansen**

An optical and irreversible temperature sensor (e.g., a time-temperature integrator) is reported based on a mechanically embossed chiral-nematic polymer network. The polymer consists of a chemical and a physical (hydrogen-bonded) network and has a reflection band in the visible wavelength range. The sensors are produced by mechanical embossing at elevated temperatures. A relative large compressive deformation (up to 10%) is obtained inducing a shift to shorter wavelength of the reflection band (>30 nm). After embossing, a temperature sensor is obtained that exhibits an irreversible optical response. A permanent color shift to longer wavelengths (red) is observed upon heating of the polymer material to temperatures above the glass transition temperature. It is illustrated that the observed permanent color shift is related to shape memory in the polymer material. The films can be printed on a foil, thus showing that these sensors are potentially interesting as time-temperature integrators for applications in food and pharmaceutical products.

1. Introduction

In the past, a variety of optical temperature sensors based on liquid crystalline materials were proposed. Typically, low molar weight non-reactive liquid crystals were employed and an optical effect was generated via a change in birefringence or reflection band.[1–3] Such sensors are often liquid-like (e.g., nematic) and behave as real-time sensors. However, a need persists for polymer based optical sensors that exhibit an irreversible response to temperature and/or analytes. The polymeric character of such a sensor would greatly simplify processing because, for instance, complex encapsulation procedures can be omitted. More importantly, an irreversible temperature sensor could be particularly useful in applications such as food or pharmaceutical products.[4,5]

Chiral nematic liquid crystalline (also called cholesteric liquid crystalline (CLC)) polymer networks based on crosslinked, reactive mesogens have been extensively investigated for the constructing of battery-free optical sensors.[6] In these systems, a chiral dopant is added to a nematic, reactive mesogen which induces a helical structure in the monomer mixture. The helical structure results in the reflection of circularly polarized light in the visible wavelength range which is directly related to the pitch of the helix.[7] The reflection band of the liquid crystalline monomer mixture is fixated in the polymer network,[8] and the change of the reflection band is due to swelling/shrinkage and/or loss of molecular order in the polymer film. In nearly all these cases, the optical response is reversible. Only recently we have reported on a CLC polymer salt saturated with water that could potentially act as a time-temperature integrator. However, contact with water should be avoided since the color changes in the film were reversible.[6f] The optical reversible response can be a limiting factor in specific applications. For instance, pharmaceutical and food products often have to be stored below a certain threshold temperature and sensors are required which permanently record temperatures above this threshold.[9,10]

Here, a new irreversible temperature, optical sensor is reported which is based on shape memory of a mechanically embossed chiral nematic polymer network consisting of hydrogen bonded mesogens (**Figure 1**,**2**).[11–13] The strong covalent bonds of the chemical polymer network are able to provide shape memory.[14–17] Shape memory polymers have recently attracted a lot of interest and are capable to return from a temporary deformed state to their original, permanent shape by an external stimulus, such as temperature change.[18] A large mechanical response, which is required for a large visible color change, is ensured by the supramolecular hydrogen bonded network.[19–21] The deformation and color only goes back to its original state after heating the polymer above the glass transition temperature (T_g).

D. J. D. Davies, A. R. Vaccaro, Dr. N. Herzer,
Dr. A. P. H. J. Schenning, Dr. C. W. M. Bastiaansen
Functional Organic Materials and Devices
Department of Chemical Engineering and Chemistry
Eindhoven University of Technology
Den Dolech 2, 5600 MB Eindhoven,
The Netherlands
E-mail: a.p.h.j.schenning@tue.nl; c.w.m.bastiaansen@tue.nl
Dr. S. M. Morris
Department of Engineering
University of Cambridge
9 JJ Thomson Avenue, Cambridge, CB3 0FA, UK
Prof. C. W. M. Bastiaansen
School of Engineering and Materials Science
Queen Mary, University of London
Mile End Road, London, E1 4NS, UK

DOI: 10.1002/adfm.201202774

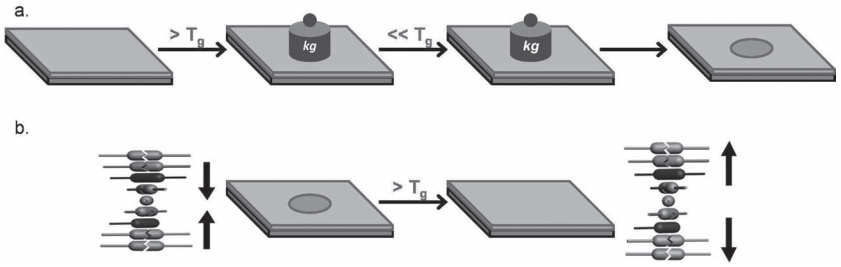

Figure 1. a) Fabrication of the irreversible temperature optical sensor by mechanical embossing. A CLC layer is embossed above the glass transition temperature (T_g) and cooled down below T_g to fixate compressive deformation together with the blue shift caused by reduction of the helical pitch. b) Sensing principle of the embossed CLC-layer. The embossed area is preserved below T_g and a permanent red shift is obtained above T_g.

2. Results and Discussion

The chiral nematic hydrogen bonded liquid crystal polymer network films were prepared as described previously.[6f] The CLC mixture contains both chemically (polymerizable acrylate groups) and physically (carboxylic acid groups which form hydrogen bonded dimers) crosslinkable groups (Figure 2a). The reactive mesogens C6M and LC756 act as chemical crosslinker and chiral dopant, respectively, while 6OBA and 6OBA-M are the H-bonding mesogens. C6BP is added to decrease the crystalline-nematic phase transition. Polymer films with a thickness of 5 to 7 μm were obtained by bar-coating the CLC mixture in THF (1:1) onto a polyimide coated rubbed glass substrate. Infrared (IR) spectroscopy measurement revealed that photopolymerization followed by thermal curing led to full acrylate conversion (Supporting Information) and a polymeric film with a narrow selective reflection band (SRB) at ≈600 nm was obtained (Figure 2b,c and Supporting Information).

Thermal and thermomechanical studies were performed using free-standing 50 μm thick polymerized CLC films, produced by capillary filling of glass cells. Differential scanning calorimetry (DSC) showed a glass transition between 40 °C and 60 °C (Supporting Information). Dynamic mechanical thermoanalysis (DMTA; **Figure 3**) revealed that the elastic modulus of the material drops from approximately 1 GPa in the glassy phase to less than 50 MPa in the rubbery phase between 40 °C and 60 °C, and that $T_g \approx 50$ °C.

The hydrogen bonded network is hardly affected by heating up to 60 °C, as revealed by IR spectroscopy monitoring the

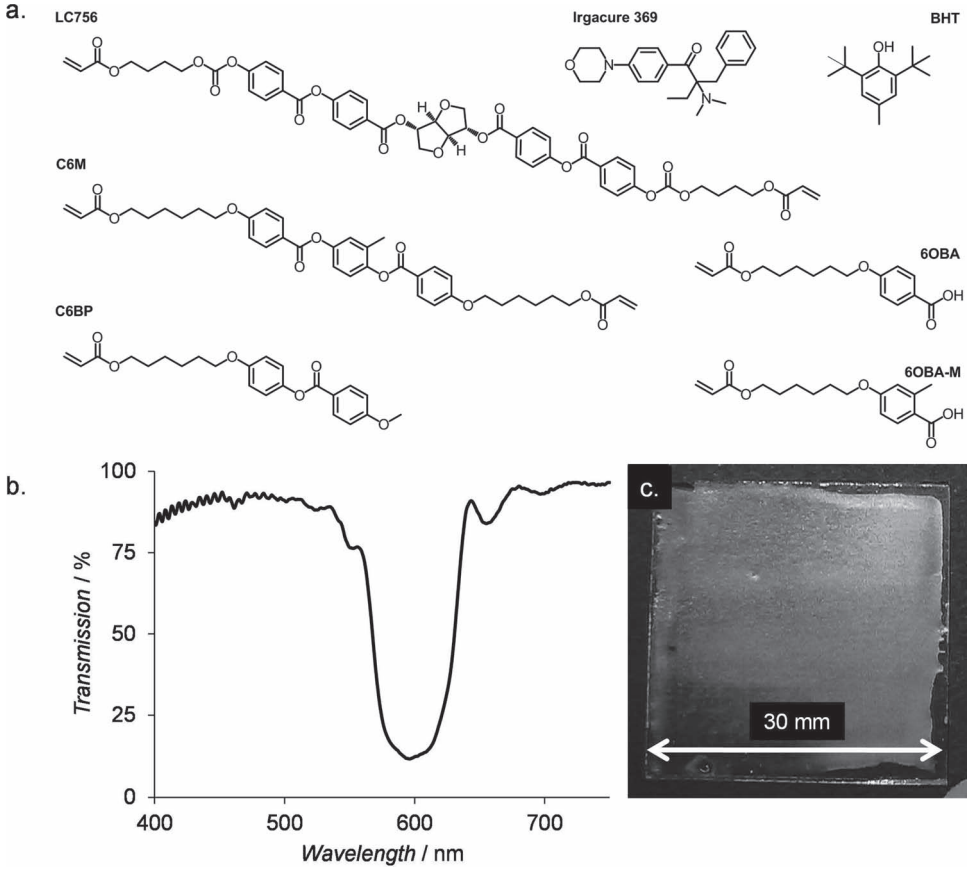

Figure 2. The CLC polymeric network. a) Chemical composition of the reactive mesogenic mixture: 6OBA, 21.9 wt%; 6OBA-M, 21.9 wt%; LC756, 4.5 wt%; C6BP, 38 wt%; C6M, 13 wt%; photoinitiator (Irgacure 369), 0.6 wt%; and 0.1 wt% of inhibitor (BHT, 3,5-di-t-butyl-4-hydroxytolueen). b) The reflection band of the polymer cholesteric network, measured with circularly polarized light. c) A photograph of the bar-coated polymer film showing an orange reflection.

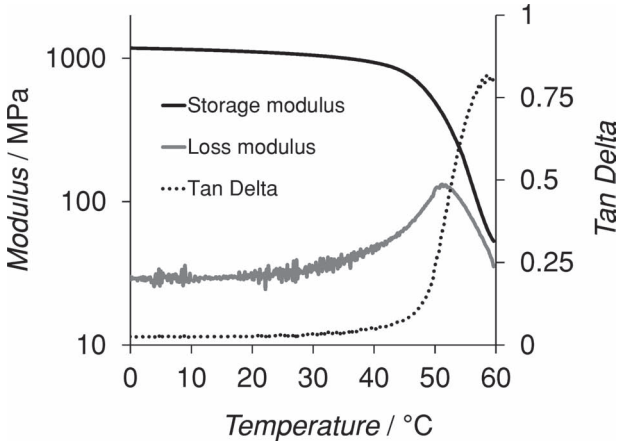

Figure 3. DMTA analysis of the polymer CLC network.

asymmetric carbonyl vibration manifested by hydrogen bonded carboxylic acid groups (Supporting Information). Upon heating above 60 °C, a gradual weakening of hydrogen bonded network strength is observed. It is also shown that residual hydrogen bonded carboxylic acid groups are present even at 180 °C.

The CLC films are mechanically embossed above T_g (60 °C) using a rigid sphere as a stamp (r = 8 mm).[22] Typically, a static load of 2.5 kg was used. After embossing at elevated temperatures, the film was slowly cooled to room temperature and the metal sphere was removed (Figure 1a). The mechanical embossing creates a spherical indentation that exhibits a color shift from orange to green, that can be observed by the naked eye and by optical microscopy (**Figure 4**a–c). The embossed regions had a radius between 0.2 and 0.25 mm. Interferometry measurements showed that the maximal indentation found in the center of the indentation is 5–10% (Supporting Information). As indicated by IR spectroscopy, the mechanical deformation was accompanied by higher average distance between hydrogen bonding units due to mechanical deformation and subsequent network fixation (Supporting Information). Most importantly, local transmission spectroscopic measurements showed that the reflection band is shifting to lower wavelengths by $\Delta\lambda$ = 30 nm (Figure 4d). This blue shift is roughly five percent ($\Delta\lambda/\lambda$ = 0.05), which is of the same order of magnitude as the indentation. As expected compressive mechanical deformation largely translates into a decrease of the pitch. The reflection band is broadened and decreases in intensity, indicating loss of the cholesteric order and/or a non-linear deformation of the pitch across the sample thickness.[22] Interestingly, these mechanically embossed films can be stored at room temperature without a change of the green reflection color.

After mechanical embossing, an optical sensor is obtained which exhibits a red shift upon heating above the glass transition temperature of the polymer. In fact, the embossed areas return to their original color, reflection wavelength, as well as original spectral width, indicating restoration of the original cholesteric pitch and the original cholesteric order (Figure 4). In addition, interferometry showed that upon heating above T_g the indentation of the embossed spherical spot flattens and a smooth film is obtained (Supporting Information). Therefore, this irreversible optical sensing of heat is attributed to a shape memory effect.

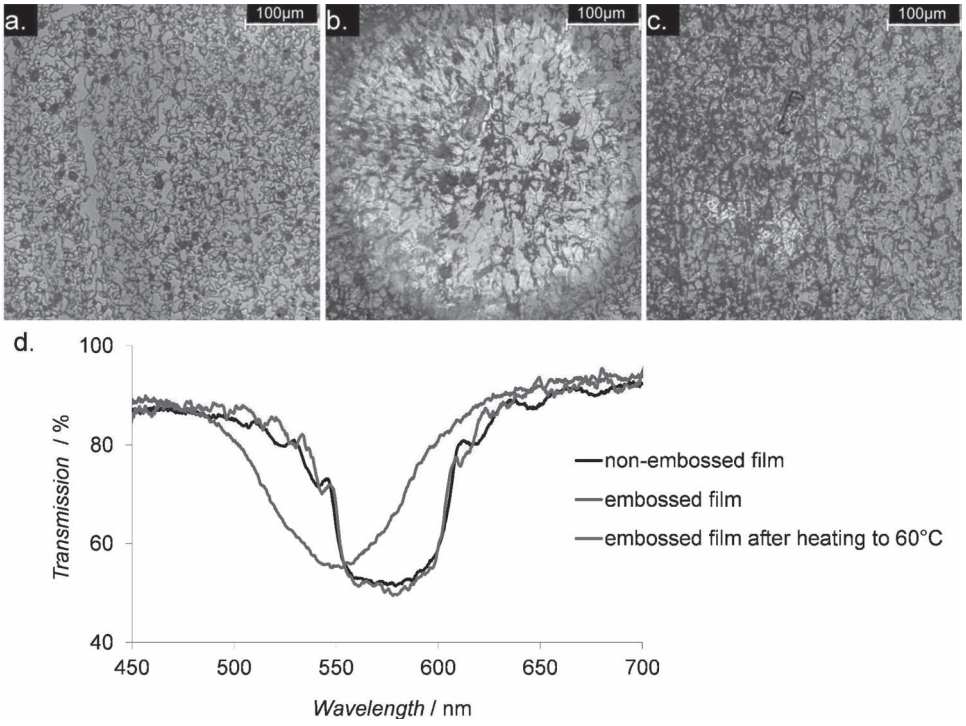

Figure 4. CLC films embossed at 60 °C with 2.5 kg load. Microscopy images recorded in reflection mode at room temperature show a) the non-embossed film, b) the embossed film, and c) the embossed film after heating to 60 °C. d) Local transmission spectra recorded at room temperature using unpolarized light.

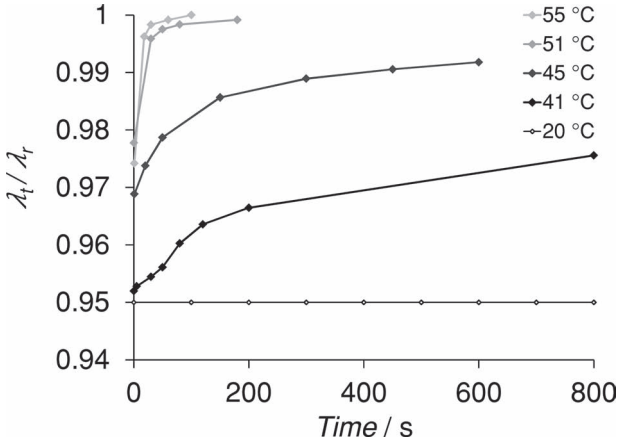

Figure 5. Time dependent sensor response at different temperatures. At $t = 0$ s, the sensor had reached the temperature set point, λ_r is the wavelength of the SRB after heating the sample to 60 °C leading to recovery of the original SRB band.

The capability of mechanically embossed CLC films to act as irreversible optical temperature sensors depends on the embossing conditions. Less load resulted in smaller indentation and less pronounced color shift, while loads being excessively higher than 2.5 kg led to fracture phenomena in the CLC film or fracture of the glass substrate. Embossing temperatures exceeding 70 °C resulted in indentations well over 10%. However, such highly deformed material was not capable of returning to the original shape (Supporting Information).

The kinetics of the optical sensor at temperatures near the glass transition temperature were evaluated by following the local reflection band (λ_t) over time under isothermal conditions. While the sensor is stable in the glassy state, a clear time- and temperature-integrating behavior could be demonstrated between 40 and 55 °C with small temperature changes inducing a large effect on the response rate (**Figure 5**). Full recovery within less than a minute was found above 50 °C, presumably due to a high degree of chain mobility. Below 50 °C, the embossed films were not fully shifted to the original color after 10 min, which correlated well with the interferometric profile of a sensor heated to 45 °C indicating partial shape recovery (Supporting Information). This kinetic behavior reveals, that a time-temperature (t-T) integrator has been constructed with a well-defined threshold temperature.

The manufacturing of low cost sensors is potentially facilitated if printing procedures can be introduced in combination with flexible substrates and roll-to-roll processing. Therefore, square patterned CLC layers were deposited on a rubbed, flexible substrate, cellulose triacetate (TAC), using inkjet printing (see Experimental Section). As ink formulation, the CLC mixture was dissolved in THF. Droplet spacing was tuned to achieve homogeneous layers with a thickness of 4 to 5 µm (**Figure 6**a). Optical microscopy images of the photopolymerized printed CLC patterns exhibited an oily streak texture and a narrow reflection band is observed in UV-vis spectra (Supporting Information) indicating a good planar alignment of the polymer film. Upon mechanical embossing, a spherical indentation is obtained with a radius of 0.35 mm, accounting for a doubled indentation area compared to embossed CLC films on glass. This increase is attributed to the deformation of the flexible TAC foil (Supporting Information). The color of the spherical indentation in the printed CLC is shifted to the blue and shows a fast and irreversible red shift when the film is heated above glass transition temperature of the polymer network (Figure 6b). These results show that printable t-T integrators can be made based on mechanical embossing.

3. Conclusions

A printable optical time-temperature integrator based on shape memory of a mechanically embossed CLC polymer network has been constructed. The sensor is capable of returning from a pitch reduction caused by shape deformation back to the original state as a function of time and temperature, which causes a visible color shift. This threshold is related to the glass transition temperature of the polymer network and, as such, it may be tunable by using other CLC mixtures. As the response of our sensor is highly interesting for time temperature devices labeling products with strict requirements on staying below a certain temperature during its entire lifetime, our concept is applicable in food packaging and medical industry. CLC layers printed on flexible foil maintain their optical sensing capability, proving the feasibility of using this system for industrial mass production based on reel-to-reel processing, which includes a whole range of device design possibilities like using patterns or assembling sensor arrays with different glass temperatures or sensing functionalities.

4. Experimental Section

Materials: C6M and C6BP were kindly provided by Merck, other materials were purchased from BASF (chiral dopant LC756), and Synthon (6OBA and 6OBA-M). The reactive components are mixed with

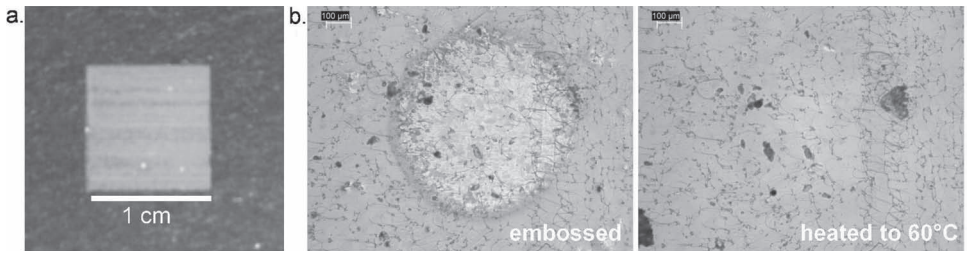

Figure 6. Inkjet printed CLC polymer film. a) Photographic image with black background. b) Microscopy images recorded in reflection mode at room temperature of a sample embossed at 60 °C with 2.5 kg load and subsequently heated to 60 °C.

0.1 wt% of inhibitor (BHT, 3,5-di-*t*-butyl-4-hydroxytolueen, Aldrich) and 0.6 wt% photoinitiator (Irgacure 369, Ciba).

Barcoated Films: Square 30 mm × 30 mm glass pieces were used as substrate. After cleaning with ethanol, ultrasonic bath (Branson 2510) and UV-Ozone photoreactor (Ultraviolet PR-100) treatment, the substrates are spincoated with polyimide (JSR grade AL24101), dried on a hot plate at 80 °C, and baked at 190 °C for 90 min. For inducing planar alignment, coated slides were rubbed on velvet cloth. The CLC mixture in THF (1:1) is bar-coated onto the slide at a coater temperature set point of 55 °C. The sample was placed on a hot plate of 80 °C for 5 min to evaporate remaining THF. The curing is executed by illumination with a high intensity EXFO lamp for 100 s under nitrogen atmosphere. This is followed by an additional post curing step of 3 h at 130 °C under nitrogen atmosphere.

Preparation of Thick Samples: The solvent free CLC mixture was heated to 80 °C and placed inside planar cells by capillary filling. Cells consisted of two polyimide-coated, velvet cloth rubbed glass sheets (antiparallel alignment), glued together using 50 µm thick spacers. Curing and post curing was done in a similar manner as the bar-coated films.

Inkjet Printing: Inkjet printing experiments on flexible substrate were performed on a Fuji Dimatix printer (DMP-2800) using 10 pL droplet size cartridges. As ink, CLC mixture in THF (1:1) was used. As substrate, TAC foil with thickness of 50 µm was used. To induce planar alignment, the TAC foil was rubbed prior to printing using a velvet cloth. As print patterns, 10×10 mm^2 squares were set with a droplet spacing of 30 µm. During printing the TAC foil was fixed on the printer table by air suction and heated to 53 °C. Deposited layers turned from scattering white to transparent orange within a few minutes. To account for more effective heat transfer through thin TAC foil than through thick glass slides, a lower temperature set-point was chosen during curing by illumination (53 °C). Apart from that, curing and post curing were done in a similar manner as the barcoated films. TAC foil maintained its shape integrity during these thermal curing conditions.

Thermal and Thermomechanical Characterization: A TA Instruments DSC Q1000 calorimeter was used to record DSC of thick samples. A TA Instruments DMA Q800 rheometer was used for DMTA analysis. Storage moduli, Loss moduli, and Tan Delta were derived from the strain response to oscillatory tensile stress (heating rate: 10 °C/min). For approximation of T_g, the onset of tan delta and the storage modulus, as well as the loss modulus was considered.

Mechanical Embossing: A Daca Tribotrack mechanical press was used, consisting of a temperature-controlled static table and temperature-controlled mobile stamp with a rigid sphere (r = 8 mm) attached to it. PDMS rubber was placed between sample and static table. To ensure conditions comparable to bar-coated glass slides, an additional glass slide was placed between TAC foil-based samples and PDMS rubber. At $T_{embossing}$ ($>T_g$) the sphere was pressed into the sample by putting a load on top of the stamp. The load was removed when the setup was cooled to room temperature.

Microscopy: A Leica CTR 6000 optical microscope was used in bright field reflection mode to monitor color shifts; in crossed polarizer transmission mode to verify planar alignment of CLC films; and in differential interference contrast (DIC) mode to visualize height profiles on blank TAC foil.

UV-Vis Spectroscopy: Determining of the global SRB position of original CLC films was done in a Shimadzu UV 3102 PC Spectroscope with circularly polarized light. Local transmission spectra on embossed areas were recorded with an Olympus BH-2 polarizing optical microscope with a resolution of 1.3 nm coupled to an Ocean Optics USB2000 Spectrometer. The light input was unpolarized.

Temperature Control: A Linkam Black TMS92 hot stage was used to control the temperature of the model system when studying the temperature dependent UV-spectra of the original film and when studying the time-temperature dependency of the height profile and the UV-Vis spectrum of the embossed area. For monitoring the heat response of TAC foil samples, a hot plate was used. To ensure reproducible heat transfer conditions despite their conical deformation after mechanical embossing, TAC foil was covered with a pre-heated glass slide.

Acknowledgements

D.J.D.D. and A.R.V. contributed equally to this work. The authors would like to thank the Stichting Innovatie Alliantie (SIA) for funding this research as part of the Raak Pro program. S.M.M. gratefully acknowledges The Royal Society for financial support.

Received: September 24, 2012
Published online: January 15, 2013

[1] C. W. Smith, D. G. Gisser, M. Young, *Appl. Phys. Lett.* **1974**, *24*, 453.
[2] M. F. Moreira, I. C. S. Carvalho, W. Cao, C. Bailey, B. Taheri, P. Palffy-Muhoray, *Appl. Phys. Lett.* **2004**, *85*, 2691.
[3] W. Hu, H. Cao, L. Song, H. Y. Zhao, S. J. Li, Z. Yang, H. J. Yang, *J. Phys. Chem. B* **2009**, *113*, 13882.
[4] B. Fu, T. P. Labuza, *J. Food Distrib. Res.* **1992**, *23*, 9.
[5] P. S. Taoukis, K. Koutsoumanis, G. J. E. Nychas, *Int. J. Food Microbiol.* **1999**, *53*, 21.
[6] For examples of H-bonded CLC-based sensors see: a) C. K. Chang, C. W. M. Bastiaansen, D. J. Broer, H.-L. Kuo, *Adv. Funct. Mater.* **2012**, *22*, 2855; b) P. V. Shibaev, R. L. Sanford, D. Chiappetta, P. Rivera, *Mol. Cryst. Liq. Cryst.* **2007**, *479*, 161; c) P. V. Shibaev, D. Chiappetta, R. L. Sanford, P. Palffy-Muhoray, M. Moreira, W. Cao, M. M. Green, *Macromolecules* **2006**, *39*, 3986; d) P. V. Shibaev, P. Rivera, D. Teter, S. Marsico, M. Sanzari, V. Ramakrishnan, E. Hanelt, *Opt. Express* **2008**, *16*, 2965; e) F. Chen, J. Guo, Z. Qu, J. Wei, *J. Mater. Chem.* **2011**, *21*, 8574; f) N. Herzer, H. Guneysu, D. J. D. Davies, D. Yildirim, A. R. Vaccaro, D. J. Broer, C. W. M. Bastiaansen, A. P. H. J. Schenning, *J. Am. Chem. Soc.* **2012**, *134*, 7608; g) C. K. Chang, C. W. M. Bastiaansen, D. J. Broer, H.-L. Kuo, *Macromolecules* **2012**, *45*, 4550.
[7] a) R. Eelkema, B. L. Feringa, *Org. Biomol. Chem.* **2006**, *4*, 3729; b) T. J. White, M. E. McConney, T. J. Bunning*J. Mater. Chem.* **2010**, *20*, 9832.
[8] J. Lub, D. J. Broer, R. T. Wegh, E. Peeters, B. M. I van der Zande, *Mol. Cryst. Liq. Cryst.* **2005**, *429*, 77.
[9] B. Fu, T. P. Labuza, *J. Food Distrib. Res.* **1992**, *23*, 9.
[10] P. S. Taoukis, K. Koutsoumanis, G. J. E. Nychas, *Int. J. Food Microbiol.* **1999**, *53*, 21–31.
[11] For a recent review on functional polymer networks based on hydrogen bonded liquid crystals see: D. J. Broer, C. M. W. Bastiaansen, M. G. Debije, A. P. H. J. Schenning, *Angew. Chem. Int. Ed* . **2012**, *51*, 7102.
[12] CLC elastomers have been mechanically deformed by uniaxial strain, see for example: a) P. Cicuta, A. R. Tajbakhsh, E. M. Terentjev, *Phys. Rev.* **2002**, *65*, 051704; b) P. Cicuta, A. R. Tajbakhsh, E. M. Terentjev, *Phys. Rev.* **2004**, *70*, 011703.
[13] For a review and issue on mechanoresponsive luminescent materials see a) Y. Sagara, T. Kato, *Nat. Chem.* **2009**, *1*, 605; b) C. Weder, *J. Mater. Chem.* **2011**, *21*, 8235.
[14] M. Behl, A. Lendlein, *Soft Mater.* **2007**, *3*, 58.
[15] H. Qin, P. T. Mather, *Macromolecules* **2009**, *42*, 273.
[16] I. A. Rousseau, P. T. Mather, *J. Am. Chem. Soc.* **2003**, *125*, 15300.
[17] K. M. Lee, T. J. Bunning, T. J. White, *Adv. Mater.* **2012**, *24*, 2839.
[18] M. Behl, R. Marc, Y. Muhammad, A. Lendlein, *Adv. Mater.* **2010**, *22*, 3388.
[19] R. V. Tal'roze, A. M. Shatalova, G. A. Shandryuk, *Polym. Sci.* **2009**, *51*, 57.
[20] G. A. Shandryuk, S. A. Kuptsov, A. M. Shatalova, N. A. Plate, R. V. Talroze, *Macromolecules* **2003**, *36*, 3417.
[21] V. S. Merekalov, S. A. Kuptsov, G. A. Shandryuk, R. V. Talroze, V. S. Bezbodorov, E. M. Terentjev, *Liq. Cryst.* **2001**, *28*, 495.
[22] As opposed to the use of a flat stamp aiming at ideal uniform layer thickness decrease, using a spherical stamp avoids practical planarization problems and leads to non-uniform, but regular layer thickness decrease.